geoconvention
Calgary • Canada • May 15-17 2023

Recurrent neural networks for DAS time-lapse imaging at CaMI Field Research Station

Jorge E. Monsegny[1], Donald C. Lawton[1,2], Daniel O. Trad[1]
[1] University of Calgary [2] Carbon Management Canada

Summary

Prior to injecting CO_2 in a carbon capture facility, a baseline seismic survey is recorded, and after some CO_2 injection, a second survey, the monitor, is also recorded. The difference between these two surveys must be related to the CO_2 injection. However, other effects can produce spurious differences that mask the CO_2 related one. In this extended abstract we test a set of recurrent neural networks to minimize these spurious differences while keeping the differences related to CO_2 injection. We also test convolutional neural networks as a base case to improve with the recurrent ones. We found that long short-term neural networks and the simple recurrent neural networks perform the best with data from CaMI-Field Research Station.

Theory

Seismic time-lapse imaging for CO_2 monitoring requires the subtraction of two seismic vintages: the baseline and the monitor. The monitor is recorded after some CO_2 has been injected and the seismic difference should be related to this CO_2. However, the different conditions of the environment can create spurious differences between the two seismic vintages. That is why some shaping filtering is applied to one of the vintages, usually the monitor, to make it the more similar to the baseline in the area outside the reservoir.

Prior to this work, time-lapse imaging was successfully performed at CaMI-FRS with geophone data (Kolkman-Quinn and Lawton, 2022). However, the CO_2 plume observed in the geophone data was not visible in the distributed acoustic sensing (DAS) data. Several theories about this were that the DAS data was not sensitive enough or that the CO_2 related anomalies were buried below the noise. For this reason, we experiment with some recurrent neural network architectures to see if they can decrease the dissimilarities outside the reservoir zone and maintain the CO_2 related differences.

We used three types of neural networks to match the monitor traces to the baseline traces: convolutional, simple recurrent and long short term memory (LSTM) neural networks. During training the number of samples is constrained to a depth above the expected reservoir where the neural networks will learn about differences not related to CO_2 injection. After training, the different neural networks are applied to the whole traces, so they undo differences not related to CO_2 injection, unmasking only the CO_2 related differences.

The first type of neural networks we tested are the convolutional neural networks (Chollet, 2021). They work like a convolution filter in signal analysis theory with its coefficients determined by the neural network training algorithm. The most well-known convolutional neural networks are 2-

dimensional due to their application in computer vision but there also exists the 1-dimensional version that we use here.

The left part of Figure 1 shows a schematic diagram of a 1-d convolutional neural network. The squares in the middle are a list of coefficients that form the kernel, and this kernel is convolved with the input trace to obtain a filtered value. A bias vector, that is not depicted in the figure, can also be added to the result. The filtered value is passed through an activation function σ to obtain one sample of the output trace.

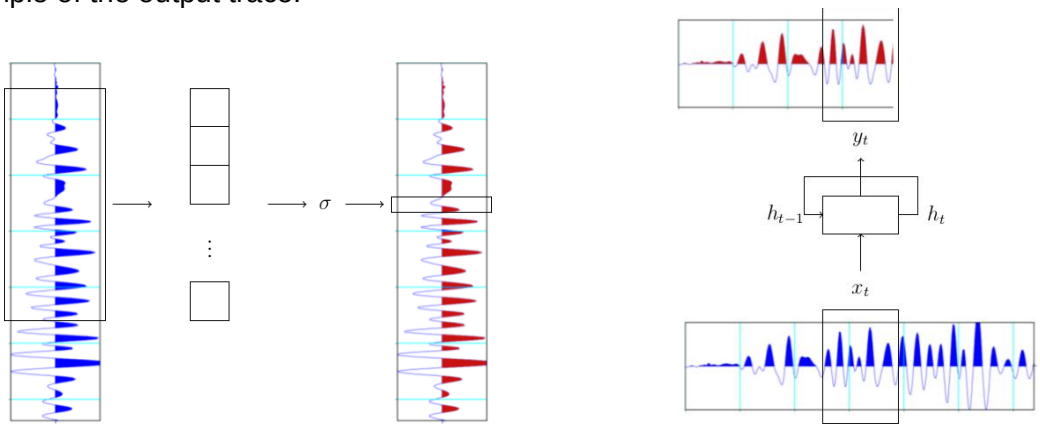

Figure 1. On the left is a 1-d convolutional neural network. ON the right is a recurrent neural network.

The second type of neural networks that we tested were the recurrent neural networks (Chollet, 2021). They work like the convolutional neural networks analyzing a small window of the input each time, but they also pass information about the current window to itself for the analysis of the next window of data. This information is the internal state of the recurrent neural network and is extremely useful for time series analysis.

The right part of Figure 1 depicts a general recurrent neural network as a black box. The input is divided into windows x_t and the network produces a window of the output y_t. In addition, information h_{t-1} from the application of the network to the previous window x_{t-1} is also used. This information is called internal state and an updated version of it, h_t, is produced for the network application to the next window x_{t+1}. The recurrent neural networks we test are two: simple recurrent and long short term memory neural networks.

The left part of the Figure 2 displays a simple recurrent neural network (Chollet, 2021). The input, output and internal state are the same as shown before. The input window x_t goes into a dense layer W_x . The internal state h_{t-1} also goes to a dense layer W_h. There is also an optional bias vector b. They are all summed up and the result is feed to an activation function σ. The result is both the output window y_t and the updated internal state h_t.

Long short term memory (LSTM) neural networks are also recurrent neural networks with a more complex inside part (Chollet, 2021). The right part of Figure 2 shows the internal structure of a LSTM. It is more complex than the previous network, so we recommend consulting Chollet, 2021 to get more detailed information. One significant difference with respect to simple recurrent neural networks is the internal state. A LSTM can remember information from the distant past more easily than a simple recurrent network due to their internal structure and memory.

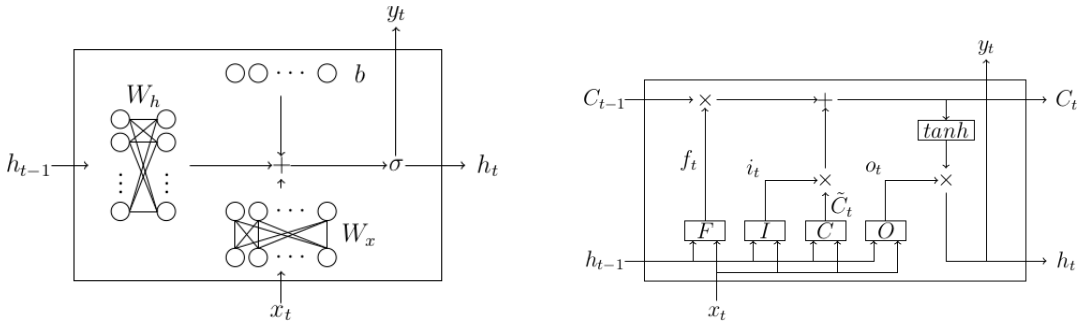

Figure 2. On the left is the internal structure of a simple recurrent neural network. On the right is the internal structure of a long short term memory (LSTM) neural network.

Results

We applied the neural networks described in the previous section to two RTM vintages form a DAS VSP time lapse survey recorded at CaMI Field Research Station. The line is the number 13 recorded twice in 2017 and 2021. Figure 3 shows the plan and profile views of this survey. In the plan view, the asterisks are the shot positions on the surface, while the o symbol is the observation well position where the DAS fibre is. The shots were made with an EnviroVibe with no more than a metre distance difference between shot positions of the two vintages.

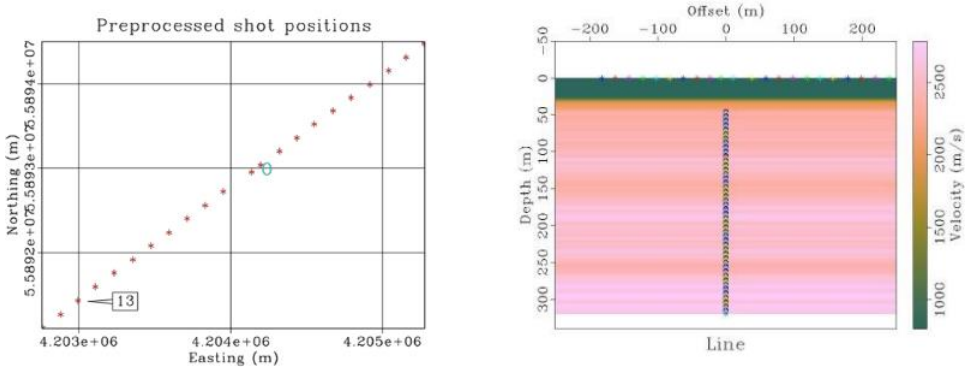

Figure 3. On the left is a plan view of the VSP line 13 at CaMI Field Research Station. The asterisks are the shot positions, and the “o” is the well head. On the right is the velocity model with VSP DAS channels.

The profile view on the same figure shows the velocity model with the shot positions on the surface as asterisks. The well is shown with circles in the middle going from 50m to 320m. The reservoir zone is around 300m depth close to the observation well.

The reverse time migration (RTM) images were created with an acoustic technique using the velocity model of Figure 3 (Monsegny, 2021). The artifacts are the product of end of line effects and variable velocities in the near surface not accounted for. We expect these artifacts to be the same on baseline and monitor images and cancel out in the subtraction.

All neural networks were trained in the same way. We paired each trace in the baseline RTM image with its corresponding trace in the monitor image. Then we shuffled the data randomly, but deterministically using the same fixed pseudo random seed in every experiment. The first half is used for training, the next quarter for validation during training and the last quarter for testing after training.

For training the traces were cut below 200m where there is not expected a CO_2 related difference. All traces were also normalized with respect to the maximum absolute value amplitude in both baseline and monitor RTM images. Neural networks work better when the data is normalized (Chollet, 2021), and we also keep the relative amplitudes between both images that is important for time lapse studies.

Other important training parameters were the learning rate equal to 0.002, the batch size equal to 32 traces, the loss function is the mean squared error and the optimization algorithm is the adaptative moment estimation or Adam.

Figure 4 shows the results after applying the different neural networks. In the figures the central vertical line is the VSP well position and the magenta one is the CO_2 injection well. Part a) is the RTM difference without shaping. Part b) is the result after using a two layered convolutional neural network. Parts c) and d) correspond to the simple recurrent neural network. The difference is that in d) two recurrent neural networks were stacked vertically. Parts e) and f) are the results for the LSTM neural networks. As with recurrent networks, the difference is that in f) two LST are stacked vertically. All the neural network results show an improvement over the original time lapse result. The events above the reservoir zone are mitigated while the CO_2 is preserved and better defined laterally.

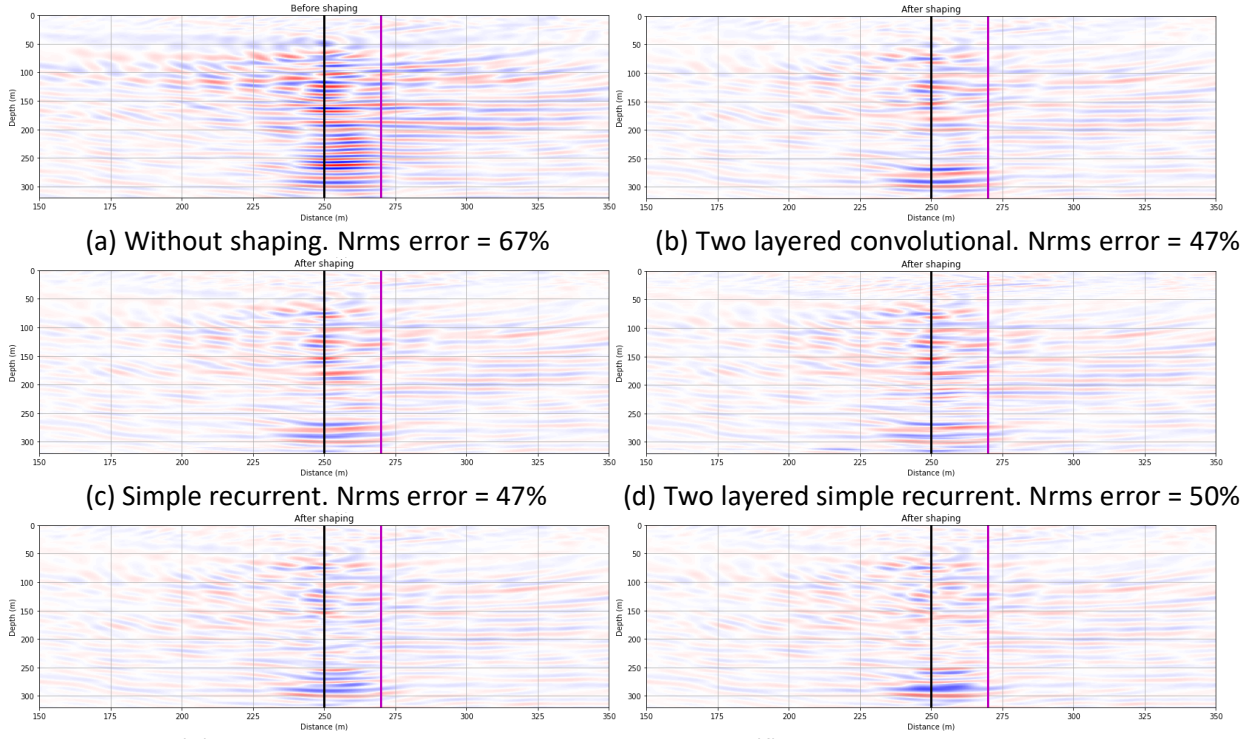

(a) Without shaping. Nrms error = 67%

(b) Two layered convolutional. Nrms error = 47%

(c) Simple recurrent. Nrms error = 47%

(d) Two layered simple recurrent. Nrms error = 50%

(e) LSTM. Nrms error = 43%

(f) Two layered LSTM. Nrsm error = 41%

Figure 4. Reverse time migration differences between monitor and baseline. The black line in the center is the position of the VSP well. The magenta line is the approximate position of the CO_2 injection well.

Figure 4 also shows the normalized mean squared (Nrms) error as a quantitative measure of the time lapse imaging results. All the neural network results decreased this error.

Conclusions

All the neural networks tested were able to decrease the original nrms error. With a couple of exceptions recurrent neural networks performed better than recurrent and lstm networks better than the recurrent ones. Also, stacking two neural networks also helped to diminish the nrms error.

Acknowledgements

We thank the sponsors of CREWES for their continued support. This work was funded by CREWES industrial sponsors and NSERC (Natural Science and Engineering Research Council of Canada) through the grant CRDPJ 543578-19. Research at the CaMI field site is supported in part by the Canada First Research Excellence Fund, through the Global Research Initiative at the University of Calgary and the CaMI.FRS Joint Industry Project. The first author (JM) is also supported by Canada First Research Excellence Fund, through the Global Research Initiative at the University of Calgary.

References

Chollet, F., 2021, Deep learning with Python: Manning Publications Co. LLC, Shelter Island, New York, second edition. Edn.

Kolkman-Quinn, B. J., and Lawton, D. C., 2022, Detection threshold of a shallow CO2 plume with VSP data from the CaMI Field Research Station: SEG Technical Program Expanded Abstracts 2022, 534–537

Monsegny, J.E. et Al., 2021, Reverse time migration approaches for DAS VSP data: Geoconvention Technical Program Expanded Abstracts 2021.